

A Mean-field Calculation for the Three-Dimensional Holstein Model¹

Chuan Liu^a and Qiang Luo^{a,b}

^a*School of Physics
Peking University*

Beijing, 100871, P. R. China

^b*State Key Laboratory for Mesoscopic Physics
Peking University*

Beijing, 100871, P. R. China

Abstract

A path integral representation appropriate for further Monte Carlo simulations is derived for the electron-phonon Holstein model in three spatial dimensions. The model is studied within mean-field theory. Charge density wave and superconducting phase transitions are discussed.

Key words: Holstein model, mean-field theory, order parameter.

PACS: 75.10.Jm, 71.10.Fd, 71.10.Li, 74.20.Mn, 74.72.-h

1 Introduction

The $BaPb_{1-x}Bi_xO_3$ alloys [1] are notable ancestors to the high temperature superconducting cuprates [2,3]. These compounds exhibit superconductivity in the Pb-rich composition range $0.05 \leq x \leq 0.3$, with a maximum $T_c \approx 13K$ near $x \approx 0.25$. A metal-semiconductor transition is observed at $x \approx 0.35$, with the semiconducting behavior continuing to the end-member compound $BaBiO_3$ [1].

By substitutional K doping at the A(Ba) site, $Ba_xK_{1-x}BiO_3$ [4] has been found to exhibit superconductivity with $T_c \approx 30K$. Band-structure calcula-

¹ This work is supported by the National Natural Science Foundation of China under Grant No. 90103006 and Grant No. 10235040 (C.L.), and the Foundation for University Key Teachers by the Ministry of Education of China (Q.L.).

tions [4,5] indicate that the conduction bands in both materials consist of σ -antibonding combinations of (Pb,K)-Bi(6s) and O(2p) states. These bands are gradually filled in rigid-band fashion with increasing x until they are half filled in $BaBiO_3$. Here, a combination of Fermi-surface nesting and the strong coupling of the conduction-band states near E_F to bond-stretching O displacements leads to a commensurate charge-density-wave (CDW) order, thereby opening a semiconducting gap at E_F , explaining the semiconducting behavior of $BaBiO_3$. The conduction bands may be well represented by simple tight-banding models. In contrast to the cuprate high temperature superconductors, these materials are three-dimensional and copper-free, rendering magnetic mechanisms inapplicable. Furthermore, conduction electrons couple strongly to breathing type oxygen phonons over a wide composition range.

It appears to us from this picture that the three-dimensional Holstein Hamiltonian on a cubic lattice might constitute a microscopic model for these materials. The Holstein Hamiltonian is:

$$H = -t \sum_{\langle \mathbf{x}\mathbf{y}\rangle, \sigma} (c_{\mathbf{x}\sigma}^\dagger c_{\mathbf{y}\sigma} + c_{\mathbf{y}\sigma}^\dagger c_{\mathbf{x}\sigma}) + \sum_{\mathbf{x}} [g(b_{\mathbf{x}}^\dagger + b_{\mathbf{x}}) - \mu] n_{\mathbf{x}} + \omega_0 \sum_{\mathbf{x}} b_{\mathbf{x}}^\dagger b_{\mathbf{x}}. \quad (1)$$

Here, $c_{\mathbf{x}\sigma}^\dagger$ creates an electron of spin σ at site \mathbf{x} , and $b_{\mathbf{x}}^\dagger$ is the creation operator for a local phonon mode of bare frequency ω_0 located at site \mathbf{x} . The electrons have a one-electron overlap t between near-neighbor sites on a cubic lattice, μ is the chemical potential and g is the electron-phonon coupling constant.

For $g = 0$, the free electrons in the three-dimensional Holstein model have a tight binding band structure: $\epsilon(\mathbf{k}) = -2t(\cos k_1 + \cos k_2 + \cos k_3)$. It has perfect nesting only at half-filling. As noted above, this band structure describes $BaPb_{1-x}Bi_xO_3$ and $Ba_xK_{1-x}BiO_3$ quite well. The Einstein phonon in the Holstein model corresponds to the oxygen breathing mode phonon in real materials. When x increases, the rigid-band fashion filling of $BaPb_{1-x}Bi_xO_3$ and $Ba_xK_{1-x}BiO_3$ corresponds to the variation of the chemical potential μ in the Holstein model which determines band filling. All these features indicate the connections between the Holstein model and these real materials. It should be noted that the boson in the Holstein model could also represent an "exciton", a "plasmon", or any other intermediate bosons. The Holstein model therefore has a wider range of applicabilities.

The idea that a single Hamiltonian (1) describes both the semiconducting and superconducting phases of $BaPb_{1-x}Bi_xO_3$ and $Ba_xK_{1-x}BiO_3$ is very appealing. The basic electron-electron interaction arising from the exchange of phonons is given by

$$V(i\omega_m) = -\frac{2g^2\omega_0}{\omega_m^2 + \omega_0^2} \quad (2)$$

with $\omega_m = 2m\pi T$. In the limit $\omega_0/t \gg 1$ with g^2/ω_0 finite, the Holstein model goes over to a negative- U Hubbard model with an effective U equal to $-2g^2/\omega_0$ [6]. Whereas the basic electron-electron interaction in a Hubbard model is instantaneous and local, as is characterized by a constant U , that in the Holstein model is retarded, i.e., $V(i\omega_m)$ depends on frequency (see Eq. (2)). This retardation effect will play an important role in subsequent discussions.

While reports on investigations for the three-dimensional Holstein model have been rare, the two-dimensional Holstein model has been previously investigated by a number of techniques, including quantum Monte Carlo simulations [6]. Some of the conclusions from these studies are expected to hold in three dimensions. According to these studies, two competing types of correlations exist in the Holstein model, s -wave superconducting and Peierls CDW. At and near half-filling, CDW long range order prevails, further away from half-filling, s -wave superconductivity dominates. As ω_0/t increases, the boundary separating CDW and superconducting phases moves toward half-filling. In the negative U Hubbard model, which is a limiting case of the Holstein model, CDW can only be stabilized at half-filling. It is interesting to note that as ω_0/t is reduced and retardation becomes important, a region of filling around the half-filled band is dominated by CDW correlations. It is reasonable to assume that a CDW phase is insulating. We thus expect that, unlike the Hubbard model, an insulating (semiconducting) phase can be stabilized away from half-filling due to retardation in the Holstein model.

As pointed out by Mattheiss and Hamann [5], the mechanism by which the semiconducting properties of $BaPb_{1-x}Bi_xO_3$ and $Ba_xK_{1-x}BiO_3$ are extended over intermediate range of compositions is less well understood. The semiconducting behavior at half-filling, i.e., $BaBiO_3$, may be understood from a combination of Fermi-surface nesting and strong coupling to breathing mode oxygen phonons. Both ingredients are necessary to open a semiconductor gap at the Fermi surface. The gap should disappear quickly with the loss of Fermi surface nesting away from half-filling. Weber [7] proposed that this semiconducting behavior was due to a combination of static incommensurate “breathing-type” charge density waves and chemical “ordering waves” on the Pb-Bi sublattice. This mechanism, however, has some difficulties with band-structure calculations and perturbative arguments [5].

It thus appears from these discussions that retardation in the Holstein model might be responsible for the stabilization of the semiconducting behavior away from half-filling. $Ba_xK_{1-x}BiO_3$ simply has a phonon frequency higher than that of $BaPb_{1-x}Bi_xO_3$. Consequently, the metallic regime of these alloys is extended closer to half-filling, where the deformation potentials for breathing-type O displacements and the electron-phonon interaction are at maximum, thus resulting in a higher T_c . As superconductivity occurs near a CDW transition, the coherence length is expected to be short, in agreement with exper-

imental observations.

Several previous studies [8,9] have used certain types of negative- U Hubbard models to describe $BaPb_{1-x}Bi_xO_3$ systems. The CDWs in Hubbard and Holstein models differ in one respect. CDW in the former is complete in the sense that alternating lattice sites are doubly occupied and empty; while in the latter, charge is only partly transferred with an amount set by retardation. Infrared [11] and x-ray-photoemission-spectroscopy [12] measurements suggest only marginal differences in the charge distributions at the Bi sites [5], lending further support to the Holstein model description of these materials.

Symmetry arguments [10] can be used to classify electronic phase transitions in the three-dimensional Holstein model. At half-filling, superconducting and CDW channels are degenerate. In this case the two-component superconducting order parameter (complex scalar) and the one-component CDW order parameter (real scalar) may be considered jointly as a three-component vector order parameter. Away from half-filling the degeneracy between the superconducting and CDW phases is broken. Thus phase transitions of CDW at half-filling, away from half-filling, and superconductivity belong to the universality classes of the three-dimensional Heisenberg, Ising, and XY models respectively. The corresponding phase transitions in $BaPb_{1-x}Bi_xO_3$ and $Ba_xK_{1-x}BiO_3$ are thus identified. It will be interesting to explore consequences of this classification in these systems.

2 Path integral representation of the model

To obtain a path integral representation for the (grand) canonical partition function $\Xi = Tr \exp[-\beta H]$, one first expresses the bosonic creation and annihilation operators in terms of a bosonic field $\Phi_{\mathbf{x}}$ and the corresponding conjugate momenta $\Pi_{\mathbf{x}}$ defined as:

$$b_{\mathbf{x}} = \sqrt{\frac{\omega_0}{2}} \left(\Phi_{\mathbf{x}} + i \frac{\Pi_{\mathbf{x}}}{\omega_0} \right) , \quad b_{\mathbf{x}}^\dagger = \sqrt{\frac{\omega_0}{2}} \left(\Phi_{\mathbf{x}} - i \frac{\Pi_{\mathbf{x}}}{\omega_0} \right) . \quad (3)$$

It is easy to see that $\Phi_{\mathbf{x}}$ and $\Pi_{\mathbf{x}}$ defined above satisfy the usual commutation relations: $[\Phi_{\mathbf{x}}, \Pi_{\mathbf{y}}] = i\delta_{\mathbf{x}\mathbf{y}}$. The Hamiltonian of the model now becomes:

$$H = -t \sum_{\mathbf{x}, \mu, \sigma} c_{\mathbf{x}\sigma}^\dagger (c_{\mathbf{x}+\mu\sigma} + c_{\mathbf{x}-\mu\sigma}) - \sum_{\mathbf{x}} [g\sqrt{2\omega_0}\Phi_{\mathbf{x}} + \mu] n_{\mathbf{x}} + \sum_{\mathbf{x}} \frac{\Pi_{\mathbf{x}}^2}{2} + \frac{\omega_0^2}{2} \Phi_{\mathbf{x}}^2 . \quad (4)$$

The inverse temperature $\beta \equiv 1/T$ is then divided into N_t slices in the “temporal” direction, each of size $a = \beta/N_t$. Inserting the completeness relation for the fermionic coherent states and the bosonic variables at any given time slice labeled by τ :

$$\int \prod_{\mathbf{x}} \left[d\Phi_{\tau,\mathbf{x}} \prod_{\sigma} \left(d\bar{\psi}_{\tau,\mathbf{x}\sigma} d\psi_{\tau,\mathbf{x}\sigma} \right) \right] \exp \left(- \sum_{\mathbf{x}\sigma} \bar{\psi}_{\tau+1,\mathbf{x}\sigma} \psi_{\tau,\mathbf{x}\sigma} \right) \times | \Phi_{\tau,\mathbf{x}}; \psi_{\tau,\mathbf{x}\sigma} \rangle \langle \bar{\psi}_{\tau+1,\mathbf{x}\sigma}; \Phi_{\tau,\mathbf{x}} | = 1 . \quad (5)$$

the partition function can be transformed into:

$$\Xi = \int \mathcal{D}\Phi \mathcal{D}\bar{\psi} \mathcal{D}\psi \prod_{\tau=0}^{N_t-1} \langle \bar{\psi}_{\tau}; \Phi_{\tau} | e^{-aH} | \Phi_{\tau+1}; \psi_{\tau} \rangle e^{-\sum_{\mathbf{x}\sigma} \bar{\psi}_{\tau+1,\mathbf{x}\sigma} \psi_{\tau,\mathbf{x}\sigma}} ,$$

where the bosonic and fermionic integrals are over all field components: $\Phi_{\tau,\mathbf{x}}$, $\psi_{\tau,\mathbf{x}\sigma}$ and $\bar{\psi}_{\tau,\mathbf{x}\sigma}$ with $\tau = 0, 1, \dots, N_t - 1$. In the temporal direction, periodic and anti-periodic boundary conditions are understood for the field Φ and $\bar{\psi}$, respectively.

The matrix element in the above expression can be evaluated easily using the properties of the coherent states and the fact that the temporal lattice spacing $a \sim 0$. It is convenient to introduce a re-scaled field A_x via:

$$A_x = \hat{g} \sqrt{2\omega_0} \Phi_x , \quad (6)$$

where we have used the notation x to label the four-dimensional site (τ, \mathbf{x}) , and \hat{g} is the dimensionless coupling measured by t , i.e. $\hat{g} \equiv g/t$. Similarly, we will use the notation: $\hat{\mu} = \mu/t$ and $\hat{\omega}_0 = \omega_0/t$. Finally, the partition function of the model is given by [13,14]:

$$\Xi = \int \mathcal{D}A \exp \left(- \sum_{x,y} A_x \frac{(-\hat{\partial}_0^2 + \omega_0^2 a^2)_{xy}}{4\hat{g}^2 \omega_0 a} A_y \right) \det(\mathcal{M}[A]^2) ,$$

$$\mathcal{M}[A]_{xy} = at \sum_{i=1}^3 (\delta_{x+\hat{i},y} + \delta_{x-\hat{i},y}) + [1 + at(\hat{\mu} + A_x)] \delta_{xy} - \zeta_{x_0} \delta_{x-\hat{0},y} , \quad (7)$$

where we have used $x = (\mathbf{x}, s)$ to collectively label $3 + 1$ dimensional lattice sites. The sign function $\zeta_{x_0} = \pm$ is present to insure the anti-periodic boundary condition for the fermion fields in the temporal direction.

It is noted that the real fermion matrix \mathcal{M} is *not* Hermitean. However, since the matrix \mathcal{M} is real and the up and down spin electrons share the same fermion matrix, the effective action is positive definite for *any* value of the chemical

potential. Therefore, this path integral representation for the Holstein model is suitable for Monte Carlo simulations [13,14] without the infamous “sign problem”.

3 The charge density wave phase

To perform a mean-field analysis for the possible charge density wave long range order, we assume that the effective action:

$$S_{eff}[A_x] = \sum_{x,y} A_x \frac{(-\hat{\partial}_0^2 + \omega_0^2 a^2)_{xy}}{4\hat{g}^2 \omega_0 a} A_y - 2Tr \log \mathcal{M}[A_x] , \quad (8)$$

has a minimum at the “ferrimagnetic” background field $A_x^{(MF)} = \hat{M} + (-)^{\mathbf{x}} \hat{\Delta}$, characterized by the magnetization parameter \hat{M} and the staggered magnetization parameter $\hat{\Delta}$. In this background field, the fermion matrix \mathcal{M} , which will be denoted as $\mathcal{M}^{(0)}$, has a simple block diagonal form in four-momentum space:

$$\mathcal{M}_{pq}[A^{(MF)}] \equiv \mathcal{M}_{pq}^{(0)} = [1 - e^{-ip_0} + at(\tilde{\mu} - \hat{\epsilon}_{\mathbf{p}})]\delta_{pq} + at\hat{\Delta}\delta_{q,p+Q} , \quad (9)$$

where p and q are two four-momenta, the temporal components of which being the usual fermionic Matsubara frequencies. The parameters $\tilde{\mu}$ and $\hat{\epsilon}_{\mathbf{p}}$ designate $\hat{\mu} + \hat{M}$ and $\epsilon_{\mathbf{p}}/t$, respectively, and Q equals $(0, \pi, \pi, \pi)$. As we will show shortly, a non-vanishing staggered magnetization order parameter $\hat{\Delta}$ signals a CDW phase in the system while the value of \hat{M} represents the “renormalization effect” of the chemical potential.

We decompose the scalar field A_x as:

$$A_x = A_x^{(MF)} + \mathcal{A}_x = \hat{M} + (-)^{\mathbf{x}} \hat{\Delta} + \mathcal{A}_x ,$$

and expand the effective action (8) around the mean-field solution $A_x^{(MF)}$. The fact that $A_x^{(MF)}$ being a saddle point of the effective action insures that the term linear in \mathcal{A}_x is absent in this expansion. Therefore, to second order in \mathcal{A}_x , we obtain:

$$\begin{aligned} S_{eff}[A] &= S_{eff}^{(0)}[A^{(MF)}] + S_{eff}^{(2)}[\mathcal{A}] , \\ S_{eff}^{(0)}[A^{(MF)}] &= \frac{\Omega\omega_0 a(\hat{M}^2 + \hat{\Delta}^2)}{4\hat{g}^2} - 2Tr \log \mathcal{M}[A^{(MF)}] , \\ S_{eff}^{(2)}[\mathcal{A}_x] &= Tr \left(\mathcal{M}^{(0)-1} \delta \mathcal{M} \mathcal{M}^{(0)-1} \delta \mathcal{M} \right) . \end{aligned} \quad (10)$$

This serves as our starting point for the mean-field calculation. In this paper, only the lowest order mean-field results will be studied. These results are contained in $S_{eff}^{(0)}$.

Since the mean-field fermion matrix $\mathcal{M}^{(0)}$ only couples momentum p with momentum $p + Q$, the lowest order effective action $S^{(0)} \equiv -\log \Xi^{(0)}$ can be easily obtained:

$$S_{eff}^{(0)}[A^{(MF)}] = \frac{\Omega\omega_0 a(\hat{M}^2 + \hat{\Delta}^2)}{4\hat{g}^2} - \sum_{\mathbf{p}} \log \left[\left(1 + at\tilde{\mu} - e^{-ip_0}\right)^2 - a^2 t^2 \hat{E}_{\mathbf{p}} \right] , \quad (11)$$

where we have introduced the energy spectrum in the CDW phase:

$$\hat{E}_{\mathbf{p}}^2 = \hat{\epsilon}_{\mathbf{p}}^2 + \hat{\Delta}^2 . \quad (12)$$

We therefore see that, if a non-zero solution for the order parameter $\hat{\Delta}$ exists, the energy spectrum develops an energy gap characterized by $\hat{\Delta}$.

It turns out that the summation over the temporal component p_0 in eq. (11) can be performed analytically. Therefore, we obtain:

$$S_{eff}^{(0)} = \frac{\Omega\omega_0 a(\hat{M}^2 + \hat{\Delta}^2)}{4\hat{g}^2} - \sum_{\mathbf{p}} \log \left[1 + \left(1 + at(\tilde{\mu} - \hat{E}_{\mathbf{p}})\right)^{N_t} \right] \left[1 + \left(1 + at(\tilde{\mu} + \hat{E}_{\mathbf{p}})\right)^{N_t} \right] . \quad (13)$$

In most cases, one is only concerned with the so-called continuum limit: $a \rightarrow 0$ with $N_t a = \beta$ being fixed. Then,

$$\left(1 + at(\tilde{\mu} + \hat{E}_{\mathbf{p}})\right)^{N_t} \sim \exp\left(\beta t(\tilde{\mu} + \hat{E}_{\mathbf{p}})\right) .$$

The free energy per lattice site: $f \equiv -\log \Xi / (\beta V_3)$, apart from irrelevant constant terms, is thus obtained ² to the lowest order in mean-field theory in the continuum limit:

$$f^{(0)} = \frac{\omega_0}{4\hat{g}^2}(\hat{M}^2 + \hat{\Delta}^2) - \frac{1}{V_3\beta} \sum_{\mathbf{p}} \log[\cosh(\beta t\tilde{\mu}) + \cosh(\beta t\hat{E}_{\mathbf{p}})] . \quad (14)$$

² We use V_3 to designate the number of sites of the three dimensional lattice.

The chemical potential μ is related to the total electron number via: $\langle N \rangle = \partial \log \Xi / (\beta \partial \mu)$. Using the doping fraction $x = \langle N \rangle / V_3 - 1$ and taking the continuum limit, this equation reads:

$$x = \frac{1}{V_3} \sum_{\mathbf{p}} \frac{\sinh(\beta t \tilde{\mu})}{\cosh(\beta t \tilde{\mu}) + \cosh(\beta t \hat{E}_{\mathbf{p}})} . \quad (15)$$

It is seen that the solution $\tilde{\mu}$ will have the same sign as x , in particular, at half-filling ($x = 0$), the solution to Eq. (15) is: $\tilde{\mu} = 0$.

The requirement that the background field $A_x^{(MF)}$ being a minimum of the effective action can be utilized to derive the so-called gap equations. The equation for \hat{M} yields the solution:

$$\hat{M} = 2(1+x)\hat{g}^2/\hat{\omega}_0 , \quad (16)$$

where $1+x$ is given by eq. (15), while the equation for $\hat{\Delta}^2$ in the continuum limit reads:

$$\frac{\hat{\omega}_0}{2\hat{g}^2} = \frac{1}{V_3} \sum_{\mathbf{p}} \frac{\sinh(\beta t \hat{E}_{\mathbf{p}})/\hat{E}_{\mathbf{p}}}{\cosh(\beta t \tilde{\mu}) + \cosh(\beta t \hat{E}_{\mathbf{p}})} , \quad (17)$$

At a given doping level x , one needs to use both Eq. (15) and Eq. (17) to solve for $\tilde{\mu}$ and $\hat{\Delta}$. The critical temperature $T_c = 1/\beta_c$ for the CDW phase is obtained from Eq. (17) and Eq. (15) by setting the order parameter $\hat{\Delta}$ to zero, or equivalently, by setting $E_{\mathbf{p}} = \epsilon_{\mathbf{p}}$ for a given value of x :

$$\frac{\hat{\omega}_0}{2\hat{g}^2} = \frac{1}{V_3} \sum_{\mathbf{p}} \frac{\sinh(\beta_c t \hat{\epsilon}_{\mathbf{p}})/\hat{\epsilon}_{\mathbf{p}}}{\cosh(\beta_c t \tilde{\mu}) + \cosh(\beta_c t \hat{\epsilon}_{\mathbf{p}})} . \quad (18)$$

It is also instructive to calculate the ensemble average of the local electron number operator $n_{\mathbf{x}} \equiv \sum_{\sigma} c_{\mathbf{x}\sigma}^{\dagger} c_{\mathbf{x}\sigma}$. To lowest order in mean-field theory, it is given by:

$$\langle n_{\mathbf{x}} \rangle = 2 + 2 \langle \mathcal{M}_{\tau_0, \mathbf{x}; \tau_0+1, \mathbf{x}}^{(0)-1} \rangle .$$

Keeping a finite and after some algebra, one obtains:

$$\langle n_{\mathbf{x}} \rangle = \frac{\langle N \rangle}{V_3} + (-)^{\mathbf{x}} \frac{\hat{\omega}_0 \hat{\Delta}}{2\hat{g}^2} + O(a) = \frac{\hat{\omega}_0}{2\hat{g}^2} [\hat{M} + (-)^{\mathbf{x}} \hat{\Delta}] + O(a) , \quad (19)$$

As we claimed before, a non-vanishing order parameter $\hat{\Delta}$ opens up an energy gap in the spectrum and signals a charge density wave order in the system.

Another useful quantity to characterize the CDW phase transition is the CDW susceptibility χ_{CDW} defined by:

$$\beta\chi_{CDW} = \frac{a}{V_3} \sum_{\mathbf{x}, \mathbf{y}, \tau} (-)^{\mathbf{x}-\mathbf{y}} \langle n_{\tau, \mathbf{x}} n_{0, \mathbf{y}} \rangle . \quad (20)$$

By virtue of translational invariance, one obtains:

$$\chi_{CDW} = \frac{1}{N_t \Omega} \sum_{x, y} e^{iQ(x-y)} \langle \bar{\psi} \psi(x) \bar{\psi} \psi(y) \rangle .$$

Since the fermion propagator for up and down spins are identical, we have:

$$\chi_{CDW} = -\frac{2}{N_t \Omega} \sum_{x, y} e^{iQ(x-y)} \langle \psi(x) \bar{\psi}(y) \psi(y) \bar{\psi}(x) \rangle . \quad (21)$$

This expression can be represented in momentum space by a loop diagram. We will calculate the susceptibility in the phase where $\Delta = 0$ for simplicity. To lowest order in mean-field theory, the susceptibility is given by:

$$\chi_{CDW}^{(0)} = -\frac{2}{N_t \Omega} \sum_p \frac{1}{[1 + at(\tilde{\mu} - \hat{\epsilon}_{\mathbf{p}}) - e^{-ip_0}][1 + at(\tilde{\mu} + \hat{\epsilon}_{\mathbf{p}}) - e^{-ip_0}]} , \quad (22)$$

where we have used the fact that: $\hat{\epsilon}_{\mathbf{p}} = -\hat{\epsilon}_{\mathbf{p}+Q}$. Using similar techniques as before, the summation over p_0 can be performed analytically, and in the continuum limit, the above equation is reduced to:

$$\chi_{CDW}^{(0)} = \frac{1}{V_3} \sum_{\mathbf{p}} \left(\frac{1}{\beta \epsilon_{\mathbf{p}}} \right) \frac{\sinh(\beta \epsilon_{\mathbf{p}})}{\cosh(\beta t \tilde{\mu}) + \cosh(\beta \epsilon_{\mathbf{p}})} . \quad (23)$$

A better approximation, the Random Phase Approximation (RPA), for the CDW susceptibility can be obtained by summing over a geometric series of $\chi_C^{(0)}$ with one phonon exchange. In this approximation, the CDW susceptibility becomes:

$$\chi_{CDW}^{(RPA)} = \frac{\chi_{CDW}^{(0)}}{1 - (2\beta t \hat{g}^2 / \hat{\omega}_0) \chi_{CDW}^{(0)}} , \quad (24)$$

which becomes divergent exactly at the critical temperature T_c , as is evident by comparing with Eq. (18).

4 The superconducting phase transition

In the previous section, we have discussed the possibility of the CDW phase transition in the Holstein model. This phase transition is characterized by a long range order parameter Δ which is diagonal in electron spins. It turns out that the system also permits a phase with long range order which is off-diagonal in the space of the electron spins. This phase is the conventional BCS-type superconducting phase with Cooper pairing. To see such a phase transition, the phonon field is integrated out from the path integral representation of the partition function. Then, another set of boson fields, namely a real scalar field Φ_x , a complex scalar field Δ_x and its complex conjugate Δ_x^* , are integrated in. Introducing the four component fermion field notation:

$$\Psi_x = \begin{pmatrix} \psi_{1x} \\ \psi_{2x} \\ \psi_{1x} \\ \psi_{2x} \end{pmatrix}, \quad (25)$$

the action of the model can be written as:

$$S = \frac{1}{2} \Psi_{\alpha x} \mathcal{D}[\Delta, \Phi]_{\alpha x; \beta y} \Psi_{\beta y} + \frac{\omega_0 a}{2\hat{g}^2} \sum_x |\Delta_x|^2 + \Phi_x \left(\frac{-\hat{\partial}_0^2 + \omega_0^2 a^2}{4\hat{g}^2 \omega_0 a} \right)_{xy} \Phi_y. \quad (26)$$

where the index α and β run from 1 to 4 and the anti-symmetric fermion matrix $\mathcal{D}[\Delta, \Phi]_{\alpha x; \beta y}$ is given by:

$$\left(\begin{array}{c|cc} 0 & -at\Delta_x^* \delta_{xy} & -\mathcal{M}_{xy}^{(0)T} - \frac{\hat{\partial}_0}{\omega_0} \Phi_x \delta_{xy} & 0 \\ & 0 & 0 & -\mathcal{M}_{xy}^{(0)T} - \frac{\hat{\partial}_0}{\omega_0} \Phi_x \delta_{xy} \\ \hline & & 0 & at\Delta_x \delta_{xy} \\ & & & 0 \end{array} \right), \quad (27)$$

where the matrix $\mathcal{M}_{xy}^{(0)}$ is given by:

$$\mathcal{M}_{xy}^{(0)} = at \sum_{i=1}^3 (\delta_{x+\hat{i}, y} + \delta_{x-\hat{i}, y}) + (1 + at\hat{\mu})\delta_{xy} - \zeta_{x0} \delta_{x-\hat{0}, y}. \quad (28)$$

The effective action of the system is obtained by integrating out the fermion fields, resulting in the Pfaffian (the square root of the determinant) of the

corresponding fermion matrix $\mathcal{D}[\Delta, \Phi]$:

$$S_{eff} = \frac{\omega_0 a}{2\hat{g}^2} \sum_x |\Delta_x|^2 + \Phi_x \left(\frac{-\hat{\partial}_0^2 + \omega_0^2 a^2}{4\hat{g}^2 \omega_0 a} \right)_{xy} \Phi_y - \frac{1}{2} Tr \log \mathcal{D}[\Delta, \Phi] . \quad (29)$$

We now proceed to search for a constant mean-field solution of the type: $\Delta_x = \hat{\Delta}_{BCS}$ and $\Phi_x = \Phi_0$ which minimizes the effective action. In this case, the fermion matrix \mathcal{D} is diagonal in four-momentum space, i.e. $\mathcal{D}_{pq} = \mathcal{D}^{(0)}(p)\delta_{pq}$ and it is given by:

$$\mathcal{D}^{(0)}(p) = \left(\begin{array}{cc|cc} 0 & -at\hat{\Delta}_{BCS}^* & -\mathcal{M}^{(0)}(p)^* & 0 \\ at\hat{\Delta}_{BCS}^* & 0 & 0 & -\mathcal{M}^{(0)}(p)^* \\ \hline \mathcal{M}^{(0)}(p) & 0 & 0 & at\hat{\Delta}_{BCS} \\ 0 & \mathcal{M}^{(0)}(p) & at\hat{\Delta}_{BCS} & 0 \end{array} \right) , \quad (30)$$

with $\mathcal{M}^{(0)}(p) = 1 + at(\hat{\mu} - \hat{\epsilon}_{\mathbf{p}}) - e^{-ip_0}$. Therefore, to lowest order in mean-field theory, the effective action is found to be:

$$\begin{aligned} \frac{1}{\Omega} S_{eff}^{(0)} &= \frac{\omega_0 a}{2\hat{g}^2} |\hat{\Delta}_{BCS}|^2 + \left(\frac{\omega_0 a}{4\hat{g}^2} \right) \Phi_0^2 \\ &\quad - \frac{1}{\Omega} \sum_p \log \left[|1 - e^{-ip_0} + at(\hat{\mu} - \hat{\epsilon}_{\mathbf{p}})|^2 + (at)^2 |\hat{\Delta}_{BCS}|^2 \right] . \end{aligned} \quad (31)$$

Since the fermion contribution is independent of Φ_0 , it is immediately seen that the solution for Φ_0 is $\Phi_0 = 0$. The summation over Matsubara frequencies can be performed analytically. In the continuum limit the result is:

$$\frac{1}{\Omega} S_{eff}^{(0)} = \frac{\omega_0 a}{2\hat{g}^2} |\hat{\Delta}_{BCS}|^2 - \frac{\beta\mu}{N_t} - \frac{1}{\Omega} \sum_{\mathbf{p}} \log \left(2 + e^{-\beta E_{\mathbf{p}}} + e^{\beta E_{\mathbf{p}}} \right) , \quad (32)$$

where the spectrum $E_{\mathbf{p}}$ is given by:

$$E_{\mathbf{p}} = \sqrt{(\mu - \epsilon_{\mathbf{p}})^2 + t^2 \hat{\Delta}_{BCS}^2} . \quad (33)$$

Chemical potential μ is determined from band filling. Using the doping fraction parameter x , the chemical potential satisfies the following equation:

$$x = \frac{1}{V_3} \sum_{\mathbf{p}} \left(\frac{\mu - \epsilon_{\mathbf{p}}}{E_{\mathbf{p}}} \right) \tanh \left(\frac{\beta E_{\mathbf{p}}}{2} \right) . \quad (34)$$

It is noted that, at half-filling $x = 0$ and the solution is $\mu = 0$ due to the symmetry of $\epsilon_{\mathbf{p}}$. The superconducting energy gap $\hat{\Delta}_{BCS}$ is obtained from the

famous BCS gap equation:

$$\frac{\hat{\omega}}{\hat{g}^2} = \frac{1}{V_3} \sum_{\mathbf{p}} \left(\frac{t}{E_{\mathbf{p}}} \right) \tanh \left(\frac{\beta E_{\mathbf{p}}}{2} \right) . \quad (35)$$

The critical temperature for the superconducting phase transition is obtained by setting the BCS gap parameter $\hat{\Delta}_{BCS}$ to zero in the above equation:

$$\frac{\hat{\omega}_0}{\hat{g}^2} = \frac{1}{V_3} \sum_{\mathbf{p}} \left(\frac{t}{|\mu - \epsilon_{\mathbf{p}}|} \right) \tanh \left(\frac{\beta_c |\mu - \epsilon_{\mathbf{p}}|}{2} \right) . \quad (36)$$

The fermion propagator is given by the inverse matrix of \mathcal{D} which again is diagonal in momentum space. If we denote:

$$\langle \Psi_{\alpha x} \Psi_{\beta y} \rangle = \frac{1}{\Omega} \sum_p e^{ip(x-y)} [\mathcal{D}^{(0)}]_{\alpha\beta}^{-1}(p) , \quad (37)$$

then the matrix $[\mathcal{D}^{(0)}]^{-1}(p)$ is given by:

$$[\mathcal{D}^{(0)}]^{-1}(p) = \frac{1}{D(p)} \left(\begin{array}{cc|cc} 0 & at\hat{\Delta}_{BCS} & \mathcal{M}^{(0)}(p)^* & 0 \\ -at\hat{\Delta}_{BCS} & 0 & 0 & \mathcal{M}^{(0)}(p)^* \\ \hline -\mathcal{M}^{(0)}(p) & 0 & 0 & -at\hat{\Delta}_{BCS}^* \\ 0 & -\mathcal{M}^{(0)}(p) & at\hat{\Delta}_{BCS}^* & 0 \end{array} \right) , \quad (38)$$

with $D(p) = |\mathcal{M}^{(0)}(p)|^2 + |at\hat{\Delta}_{BCS}|^2$.

We can also calculate the superconducting susceptibility defined by:

$$\chi_{BCS} = \frac{1}{N_t \Omega} \sum_{x,y} \langle \Psi_{1x} \Psi_{2x} \Psi_{4y} \Psi_{3y} \rangle . \quad (39)$$

For simplicity, we will evaluate the superconducting susceptibility in the phase with vanishing $\hat{\Delta}_{BCS}$ (high temperature phase). After some algebra, we obtain to the lowest order:

$$\chi_{BCS}^{(0)} = \frac{1}{V_3} \sum_{\mathbf{p}} \frac{1}{\beta |\mu - \epsilon_{\mathbf{p}}|} \tanh \left(\frac{\beta |\mu - \epsilon_{\mathbf{p}}|}{2} \right) . \quad (40)$$

Under RPA, the susceptibility becomes:

$$\chi_{BCS}^{(RPA)} = \frac{\chi_{BCS}^{(0)}}{1 - (\beta t \hat{g}^2 / \hat{\omega}_0) \chi_{BCS}^{(0)}} , \quad (41)$$

which becomes divergent exactly at β_c determined by Eq. (36).

5 Results and discussions

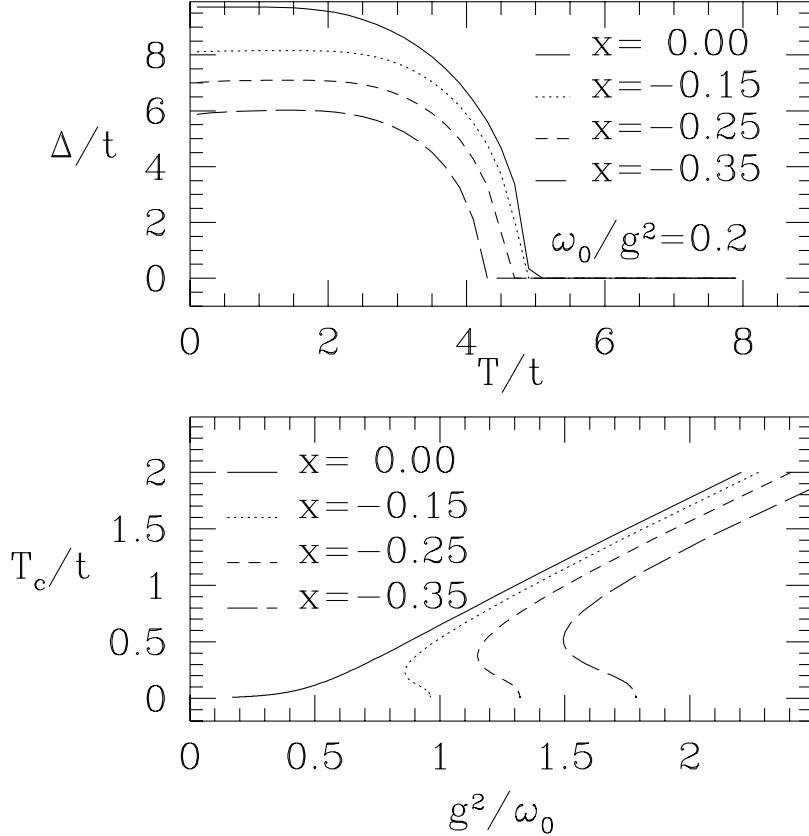


Fig. 1. In the lower half of the figure, the critical temperatures for the CDW phase transition are plotted as a function of g^2/ω_0 for four different doping levels: $x = 0.00, -0.15, -0.25, -0.35$. In the upper half of the figure, the order parameters for the CDW phase transition are plotted as a function of the temperature T/t for a given value of $\omega_0/g^2 = 0.2$ for four different doping levels: $x = 0.0, -0.15, -0.25, -0.35$.

Mean-field equations discussed in previous sections can be evaluated numerically and the results for the critical temperatures and the order parameters are summarized in Fig. 1 and Fig. 2. In the lower half of the figures, we plot the critical temperatures as a function of $\hat{g}^2/\hat{\omega}_0$ for four different doping levels: $x = 0.00, -0.15, -0.25, -0.35$. The critical temperatures for the superconducting phase transition are represented by the four lines that increase with $\hat{g}^2/\hat{\omega}_0$ near the bottom of Fig. 2. They show rather weak dependence on doping. The corresponding lines for the CDW phase transition illustrate a much stronger

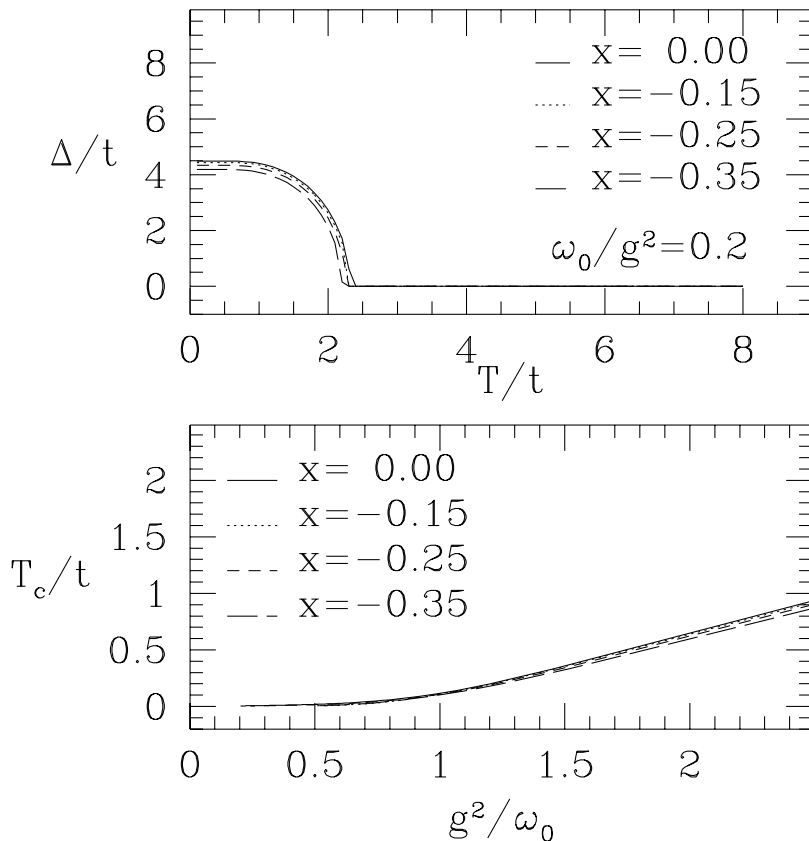


Fig. 2. In the lower half of the figure, the critical temperatures for the BCS superconducting phase transition are plotted as a function of g^2/ω_0 for four different doping levels: $x = 0.00, -0.15, -0.25, -0.35$. In the upper half of the figure, the order parameters for the BCS superconducting phase transition are plotted as a function of the temperature T/t for a given value of $\omega_0/g^2 = 0.2$ for four different doping levels: $x = 0.0, -0.15, -0.25, -0.35$.

dependence on doping compared to the superconducting critical temperatures. It is noted that, for a given value of $\hat{g}^2/\hat{\omega}_0$, the critical temperatures for the CDW phase transition decrease as the doping is increased. At exactly half filling, the critical temperature for the CDW phase transition is always higher than that of the superconducting phase transition. While the issue of the stability of the CDW and superconducting phases can only be addressed by a more sophisticated calculation, here we simply take the magnitude of the critical temperatures and order parameters as a measure of the tendency that the system is likely to be in one of these phases. Thus, we expect the system to be in a CDW phase at half filling. Away from half filling, the critical temperature for the CDW phase transition eventually becomes smaller than that of the superconducting phase transition. This is a signal that the CDW phase will eventually become unstable when the system is doped away from half filling. The superconducting phase will become dominant at low temperatures.

In the upper half of the figures, we plot the order parameters $\hat{\Delta} = \Delta/t$ for the CDW and the superconducting phase transitions as a function of temperature T/t at $\hat{\omega}_0/\hat{g}^2 = 0.2$ for the same four different doping levels. It is seen that, for a given value of $\hat{\omega}_0/\hat{g}^2$, both order parameters decrease as the doping is increased. However, the order parameter for the CDW phase decreases much more rapidly than the superconducting order parameter when the system moves away from half filling. These features indicate that the CDW phase is most favored at half filling, in agreement with our qualitative expectations discussed in the introduction.

6 Conclusions

In this paper, we present our mean-field analysis of the three dimensional Holstein model. A path integral representation of the model is obtained which is suitable for further Monte Carlo simulations. The critical temperatures and the order parameters are obtained within mean-field approximation for both the CDW phase and BCS superconducting phase transitions. Our results are consistent with the picture that the CDW phase is most favored at half-filling. Away from half filling, the usual BCS superconducting phase becomes important. Higher order calculations are necessary to further explore the competition between different electronic phase transitions.

References

- [1] A.W. Sleight, J.L. Gillson, and P.E. Bierstedt, *Solid State Commun.* **17**, 27 (1975).
- [2] J.G. Bednorz and K.A. Muller, *Z. Phys.* **B 64**, 189 (1986); J.G. Bednorz, M. Takashigi, and K.A. Muller, *Europhys. Lett* **3**, 379 (1987).
- [3] M.K. Wu, J.R. Ashburn, C.J. Torng, P.H. Hor, R.L. Meng, L. Gao, Z.J. Huang, Y.Q. Wang, and C.W. Chu, *Phys. Rev. Lett.* **58**, 908 (1987).
- [4] L.F. Mattheiss, E.M. Gyorgy, and D.W. Johnson, Jr. *Phys. Rev. B* **37**, 3745 (1988).
- [5] L.F. Mattheiss, and D.R. Hamann, *Phys. Rev. B* **28** 4227 (1983); L.F. Mattheiss, and D.R. Hamann, *Phys. Rev. Lett.* **60**, 2681 (1988).
- [6] R.T. Scalettar, N.E. Bickers, and D.J. Scalapino, *Phys. Rev. B* **40**, 197 (1989).
- [7] W. Weber, *Jpn. J. Appl. Phys.* **26**, Suppl. 3, 981 (1987)
- [8] N.E. Bickers, R.T. Scalettar, and D.J. Scalapino, *Int. J. Mod. Phys.* **B 1**, 687 (1987)

- [9] Zhang Li-yuan, Solid State Commu. **70**, 1065 (1989)
- [10] R.T. Scalettar, E.Y. Loh, J.E. Gubernatis, A. Moreo, S.R. White, D.J. Scalapino, R.L. Sugar, and E. Dagotto, Phys. Rev. Lett. **62**, 1407 (1989).
- [11] J.Th.W. de Hair and G. Blasse, Solid State Commun. **12**, 727 (1973)
- [12] G.K. Wertheim, J.P. Remeika, and D.N.E. Buchanan, Phys. Rev. B **26**, 2120 (1982)
- [13] C. Liu, Chin. Phys. Lett. **17**, 574 (2000)
- [14] X. Zhu and C. Liu, Commun. Theor. Phys., **36**, 625 (2001)